Journal of Archaeological Science 34 (2007) 830–841
http://www.elsevier.com/locate/jas

Methods for the extraction of archaeological features from very high-resolution Ikonos-2 remote sensing imagery, Hisar (southwest Turkey)

V. De Laet [a,*], E. Paulissen [a], M. Waelkens [b,1]

[a] Physical and Regional Geography Research Group, K.U. Leuven, Geo-Institute, Room 03.212, Celestijnenlaan 200 E, B-3001 Heverlee, Belgium
[b] Eastern Mediterranean Archaeology, K.U. Leuven, Blijde Inkomststraat 21, B-3000 Leuven, Belgium

Received 28 March 2006; received in revised form 8 August 2006; accepted 1 September 2006

Abstract

Archaeological research in the territory of Sagalassos is a multidisciplinary project covering scientific disciplines traditionally linked to archaeology and also new technologies such as very high-resolution remote sensing with sufficient radiometric and spatial resolution (<2.5 m). This paper focuses on the evaluation of GIS-, pixel- and object-based techniques for automatic extraction of archaeological features from Ikonos-2 satellite imagery, which are then compared to a visual interpretation of ancient structures. The study was carried out on the unexcavated archaeological site of Hisar (southwest Turkey). Although all techniques are able to detect archaeological structures from Ikonos-2 imagery, none of them succeed in extracting features in a unique spectral class. Various landscape elements, including archaeological remains, can be automatically classified when their spectral characteristics are different. However, major difficulties arise when extracting and classifying archaeological features such as wall remnants, which are composed of the same material as the surrounding substrate. Additionally, archaeological structures do not have unique shape or colour characteristics, which can make the extraction more straightforward. In contrast to automatic extraction methods, a simple visual interpretation performs rather well. The methods presented in this paper can be applied with variable success to archaeological structures composed of the same material as the surrounding substrate, which is often the case.

Keywords: Archaeology; Remote sensing; Ikonos

1. Introduction

"Remote sensing is the acquisition of information about an object without touching it" (Jensen, 2000). This broad definition encompasses all types of remote sensing, including sub-surface remote sensing, aerial photography, aerial spectroscopy and satellite remote sensing. Hence, in its broadest sense and in relation to archaeology, remote sensing encompasses methods to discover and map remnants of past civilisations above or below ground level (e.g. crop marks, buried archaeological remains, traces of ancient industrial activity and above ground architectural remnants). Remote sensing is very useful in preparing an intensive survey campaign or directing fieldwork. Viewing archaeological structures from ground level generally does not clearly identify the spatial characteristics of these structures or the relationship to surrounding archaeological sites. In some cases ancient structures are not apparent from ground level but become obvious from a bird's eye view.

Since the beginning of the 20th century, aerial photography has been used in archaeology primarily to view features on the earth's surface, which are difficult if not impossible to visualise from ground level (Sever, 1995; Vermeulen and Verhoeven, 2004). With the launch of the first Landsat satellite in 1972 (http://landsat7.usgs.gov/), satellite remote sensing also became accessible to the archaeological community (Clark et al.,

* Corresponding author. Tel.: +32 16 32 64 13/33; fax: +32 16 32 29 80.
E-mail address: veronique.delaet@geo.kuleuven.be (V. De Laet).
[1] Tel.: +32 16 32 48 62; fax: +32 16 32 50 94.

0305-4403/$ - see front matter
doi:10.1016/j.jas.2006.09.013

1998). However, due to ground resolution constraints, much of these satellite images do not provide more and probably provide even less information than aerial photography for archaeological purposes. Indeed, even the most recent Landsat ETM^{+} images have a resolution of 15 m for the panchromatic band, which is not detailed enough for the identification of most archaeological structures. Therefore, the launch of the first commercial very high-resolution satellite, Ikonos, in 1999 was a major advancement for archaeological research application purposes. This satellite platform provides panchromatic images with 1 m spatial resolution. Fusing the 1 m panchromatic and 4 m multispectral bands, a 1 m false or natural colour image can be generated. Recently, aerial hyperspectral imagery has also been used in archaeology (Emmolo et al., 2004). Hyperspectral imagery is characterised by its enormous number of wavebands and (not necessarily) very high spatial resolution defined by the operator (PCI Geomatics, 1998). Until now, very few geoarchaeological studies have applied images with such a high spatial resolution (Changlin et al., 2004; Emmolo et al., 2004; Georgoula et al., 2004; Pavlidis, 2005).

Within this study, three satellite remote sensing images with varying ground resolutions (ASTER, SPOT and Ikonos-2) are examined in order to test their potential for automatic extraction of archaeological features, by means of GIS-, pixel- and object-based methods. Subsequently the obtained results are compared with a visual interpretation.

2. Study area

The study area covers the archaeological site of Hisar, located in southwest Turkey, roughly 100 km north of Antalya (Fig. 1a, b). The Hisar site was chosen for this study because

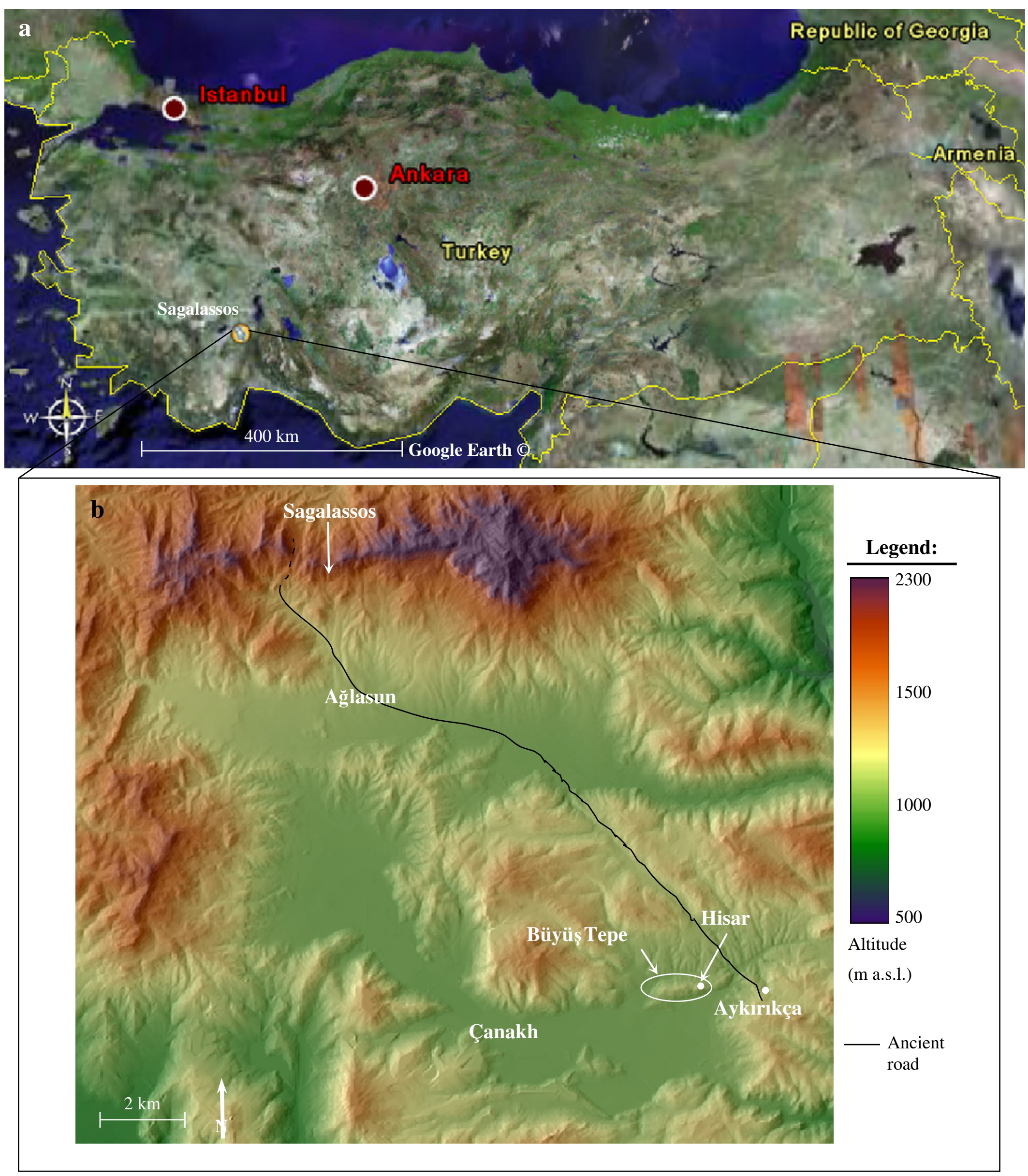

Fig. 1. Location of the study area. (a) Situation of the study area in Turkey. (b) Physical setting of the archaeological site of Hisar (20 m resolution DEM derived from 1:25,000 topographic map).

of its large size and many vertical, well visible archaeological structures. In ancient times, the Western Taurus Mountains, in which Hisar is set, was known as the region of Pisidia (Bracke, 1993).

The Hisar site is situated on an isolated hill (Büyüş Tepe, Turkish for magic hill) bordered with steep slopes—altitude between 1050 and 1200 m a.s.l—and situated 150 m above the Çanaklı plain (Fig. 2). The site, surveyed in 1993, is a well-fortified stronghold, roughly 14 km southeast of the ancient metropolis Sagalassos (Fig. 1b). Because of its heavy defence walls and the building techniques used, the site probably dates back to the Late Iron Age and early Hellenistic period (Vanhaverbeke and Waelkens, 2003). Hisar may have had an important strategic function during Hellenistic times, because of its location in the vicinity of an ancient road (Fig. 1b). Remnants of ancient houses and the Hellenistic defence wall are also depicted in Fig. 2b and c. Hisar is the successor of the Early Iron Age site Aykırıkça, located some 2 km to the east (Fig. 1b) (Waelkens et al., 1997). The substrate of the Büyüş Tepe is composed of autochthonous limestone of the Bey Dağları formation (Şenel, 1997). The site overlooks the western part of the large, fertile Çanaklı basin, filled with alluvial and colluvial deposits of Quaternary age (Fig. 1b). Today, in combination with rainfed agriculture, irrigated agriculture is only observed in the southern part of the Çanaklı plain. North of the Hisar site a mixture of rainfed agriculture and degraded *Quercus coccifera* maquis is present whereas to the east of Hisar, land cover consists of alternating *Pinus brutia* and *Pinus nigra* forests.

3. Methods

3.1. Adequate satellite imagery

Before analysing remote sensed imagery, the minimum spatial resolution necessary to detect archaeological structures under study has to be defined. The images in Fig. 3 show the Hisar site and its surroundings. They cover the same area and have the same scale, but their spatial resolution and hence their information level is quite different. ASTER images have a moderate resolution and record data in 14 spectral bands: three bands in the Visible Near InfraRed Region (VNIR) with a spatial resolution of 15 m, six bands in the Short Wave InfraRed Region (SWIR) with a spatial resolution of 30 m, and five bands in Thermal InfraRed Region (TIR) with a spatial resolution of 90 m (Abrams, 2000). The ASTER image used in this analysis is a 1B image, taken on 18 October 2001 at 09.03 am (Fig. 3a). The SPOT5 image was acquired on 5 December 2003 at 09.11 am (Fig. 3b). SPOT5 imagery has a high spatial resolution of 2.5 m for the panchromatic band, 10 m for the three VNIR wavebands and 20 m spatial resolution for the SWIR band (http://spot5.cnes.fr). Finally, a very high-resolution Ikonos-2 image taken on 8 November 2000 at 08:41 GMT is used (Fig. 3c) (©2000, Space Imaging, all

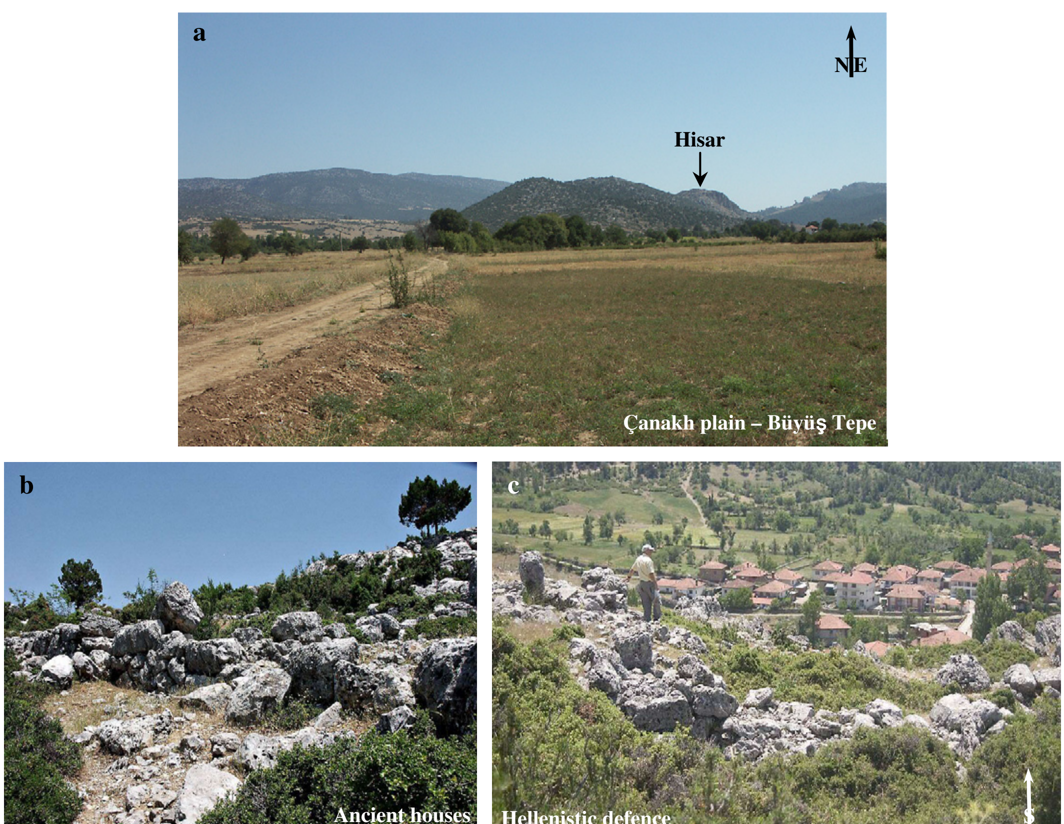

Fig. 2. (a) Büyüş Tepe seen from the south. (b, c) Archaeological structures at Hisar (photographs: survey team, Sagalassos project).

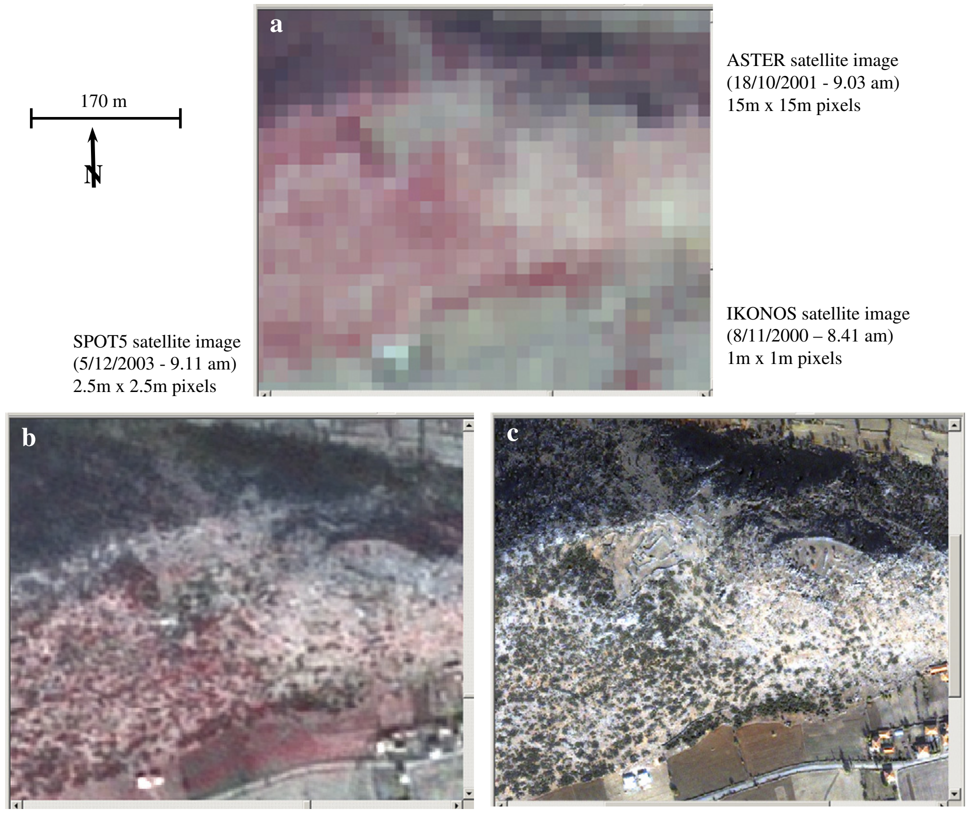

Fig. 3. The effect of spatial resolution on the visibility of archaeological structures on satellite imagery.

rights reserved). Ikonos-2 imagery, launched in 1999, contains one panchromatic band with a spatial resolution of 1 m and four multispectral bands with a spatial resolution of 4 m (Table 1) (http://www.spaceimaging.com /products /ikonos/index.htm).

A minimum spatial resolution of 1 m is required for adequate visual interpretation and inferred automatic extraction of archaeological features from remote sensed imagery, as is determined from Fig. 3. For the time being, only five types of imagery accomplish this requirement: commercial satellite imagery of Ikonos-2 and Quickbird, aerial photographs, Russian Corona imagery and aerial hyperspectral imagery. Aerial photographs and Corona imagery are photographs that do not provide any spectral information. Hence, they are omitted in this study. Since hyperspectral imagery is not at our disposal, only Quickbird and Ikonos-2 are left. In relation to this study, an Ikonos-2 image covering the Hisar site and its surroundings is used.

Preceding the automatic extraction of archaeological features from Ikonos-2 imagery, the high-resolution panchromatic and low-resolution multispectral bands are fused using an IHS (Intensity Hue Saturation) transformation in Envi® to produce a pan-sharpened colour image. This sharpened image encompasses the spectral information present in the original multispectral data, but with an effective spatial resolution of the panchromatic band (Leica, 2002). Hence, image sharpening has important implications, especially for pixel-based classifications that are entirely based on the spectral information present in the imagery. As such, pixel-based classifications are not carried out at a spatial resolution of 1 m, in the case of Ikonos imagery, but at a spatial resolution of 4 m. Consequently, the minimum spatial resolution necessary to detect archaeological features is only relevant for the panchromatic information and not for the multispectral information contained in the imagery.

Next, this pan-sharpened image is further rectified in PCI Geomatics® using ground control points derived from a 1:25,000 topographic map and the Ortho Kit supplied by the image provider, in order to get a spatial accuracy of 3 to 4 m (Fig. 7) (PCI Geomatics, 1998). With the intention not to bias the classification results, no radiometric corrections are applied.

During the acquisition process of satellite imagery, the earth's surface information is converted into digital numbers (analogue-to-digital signal conversion). When imagery of different sensors or acquisition times have to be compared, raw sensor data must be radiometrically pre-processed to derive useful information from the digital numbers produced by the sensors (Chavez, 1988; Colby, 1991; Conese et al., 1993; Crippen, 1987; Dave and Bernstein, 1982; Franklin and Giles,

Table 1
Spectral characteristics of Ikonos-2 imagery

	Bandwidth (μm)	Spatial resolution (m)
Panchromatic	0.45–0.90	1
B and 1	0.45–0.53 (blue)	4
B and 2	0.52–0.61 (green)	4
B and 3	0.64–0.72 (red)	4
B and 4	0.77–0.88 (near infrared)	4

Source: http://www.spaceimaging.com/whitepapers_pdfs/IKONOS_Product_Guide.pdf.

1995; Kaufman, 1989; Lillesand et al., 2004; Mather, 2004; Qi et al., 1993; Smith et al., 1980). Since the latter is not the case for this research, raw sensor data are used in the classification process.

3.2. Extraction of archaeological features from Ikonos-2 imagery

In the first place, a visual interpretation of the Ikonos-2 image is performed by digitising a number of the supposed archaeological structures based on shape, tone, linearity and spatial patterns between different structures as set out in Table 2.

The primary aim of this research is to evaluate the contribution of an automatic extraction of archaeological features versus a visual interpretation from very high-resolution remote sensing imagery. Therefore, three different methods are tested:

- a GIS-based method (an edge enhancement filtering technique);
- a pixel-based method (a maximum-likelihood classification);
- an object-based method (a segmentation followed by a nearest neighbourhood classification).

These methods have already been applied for the extraction and classification of various landscape elements in geology, geomorphology and ecology (Hofmann, 2001; Jordan et al., 2005; Masuoka et al., 2003), but no analogies have been described for the classification and extraction of archaeological features.

Various landscape elements can be automatically classified when their spectral characteristics are different. However, when extracting and classifying archaeological features such as remnants of walls, the major difficulty is that they are often built with materials identical to the surrounding substrate. At Hisar, the spectral characteristics of the archaeological structures and surrounding substrate are identical as both are composed of white limestone. In addition, archaeological structures do not have unique shape or spectral characteristics, which can make the extraction more straightforward. Moreover, the width and length of ancient walls are very variable and walls of this age are seldom straight. With regard to their spectral characteristics, ancient walls are often degraded by surface weathering or covered with different types of moss and lichen causing a change in reflection.

3.2.1. GIS-based method: edge enhancement filtering technique

Because no analogies for automatic archaeological feature extraction are found in the literature, filtering techniques used for automatic road extraction from high-resolution remote sensing images and filtering methods used for lineament extraction in geology are applied (Moore and Waltz, 1983; Neawsuparp and Charusiri, 2004; Richards and Xiuping, 1999). The edge enhancement filtering technique available in Idrisi® provides the best results. It accentuates areas of abrupt change in continuous surfaces and a new pixel value is derived from the original pixel value and surrounding pixel values by moving a window with a specific kernel size (3 by 3, 5 by 5 or a user specified kernel size).

3.2.2. Pixel-based method

Pixel-based methods only take into account the spectral characteristics of the pixels in the image. Various pixel-based methods (SAM, Parallelepiped, Minimum Distance, Maximum Likelihood) are evaluated and finally a maximum likelihood classification is selected, because of the incorporation of both variance and covariance of the spectral classes (Fig. 4)

Table 2
Ikonos-2 visual archaeological interpretation (modified after Pavlidis, 2005)

Attributes	Archaeological description
Tone	Tonal differences in soil may indicate buried structures (crop marks)
Texture	Different vegetation textures may indicate buried features (crop marks)
Shape	Knowledge of shape of archaeological features can assist with determining whether a feature can be recognised as archaeological or not
Size	The dimensions of the feature are also important in order to regard the feature as archaeological or not
Spatial patterns	The spatial patterns among different features may represent an ancient settlement
Orientation	Some archaeological features are consistently orientated in a certain direction
Shadows	Positive archaeological features appear in an imagery through the shadows they cast
Spatial relationships	Ruins that have been abandoned for hundreds or thousands of years are sometimes located in isolated areas. Depending on the state of the ruins, they may still be associated with other near by ancient features

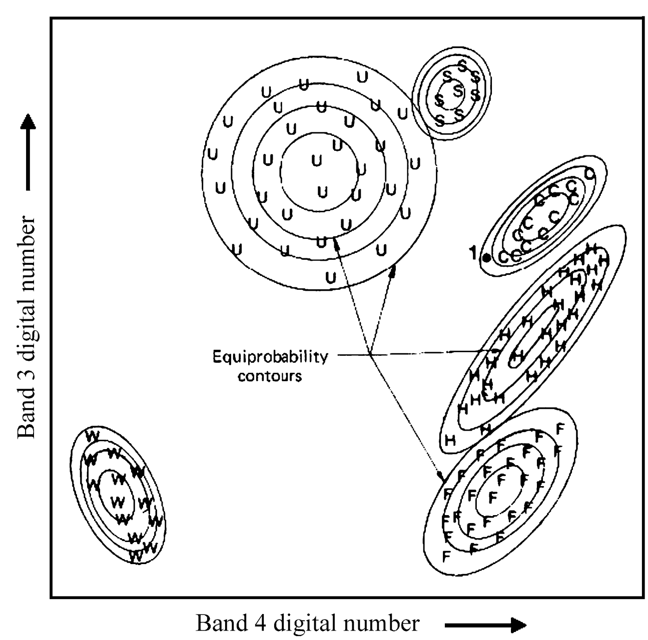

Fig. 4. Class division defined by a maximum likelihood classifier (Lillesand et al., 2004).

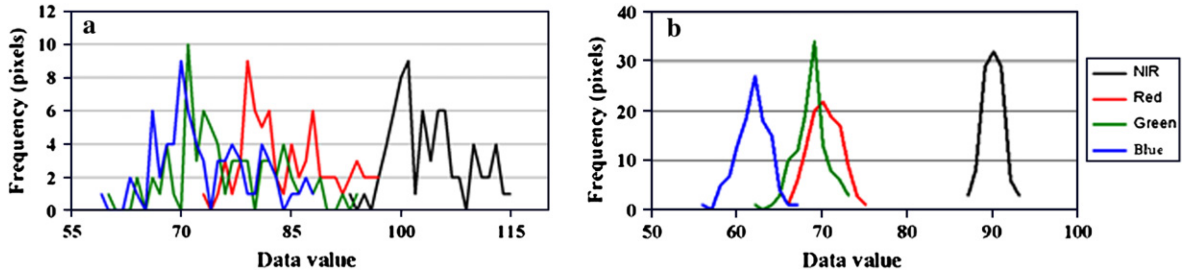

Fig. 5. Signature distribution of limestone outcrops (a) and wasteland (b).

(Lillesand et al., 2004). This classification method assigns a pixel to the class with the highest probability.

To apply a maximum likelihood classification, different types of land cover training samples are selected to guide the classification and test the class separability using the Transformed Divergence value (Swain and Davis, 1978). Training samples are selected based on field observations.

As archaeological remains of the Hisar site mainly consist of limestone walls of about 0.5–1 m high, they are also detectable by their shadows. Hence, only those two classes (walls and shadows of walls) are selected for the extraction of archaeological features.

Due to atmospheric absorption of carbon dioxide, ozone and water vapour, only the 3–5 μm, 8–9 μm and 10–14 μm regions of the thermal infrared band are useful in remote sensing (Van Der Meer and De Jong, 2003). Other pronounced absorption features are present at 1.4 and 1.9 μm. As such, these regions are not used in remote sensing of the earth's surface (Mather, 2004). Regarding the characterisation of limestone, a low contribution to the red aspect of the electromagnetic spectrum is observed. Limestone possesses typical CO_3^{2-}-ion absorption features in the 1.8–2.5 μm region, with two strong absorption features at 2.3–2.35 μm and 2.50–2.55 μm and three weaker bands at 1.85–1.97 μm, 1.97–2.00 μm and 2.12–2.16 μm (Van Der Meer and De Jong, 2003). Areas under shadow significantly modify the value of the surface signature: shadow reduces the reflectance as well as the standard deviation value of the surface reflectance (Massalabi et al., 2004).

Classification problems occur because for some land cover classes no normality can be achieved—a requirement for using a maximum likelihood classification. For instance, limestone signatures do not show a normal distribution in contrast with wasteland (Fig. 5). Except for four class-combinations, the separability index does not provide problems as all values are higher than 1.9, the critical separability threshold (Jensen, 1996). Class-combinations with values between 1.9 and 1.7 are difficult to distinguish, and it is impossible to differentiate combinations with values lower than 1.7 (Jensen, 1996).

3.2.3. Object-based remote sensing

Very often, conventional pixel-based techniques do not work very well, as a pixel is not related to the characteristics of an object or an area as a whole, but to components of it (Blaschke and Strobl, 2001). An object-based method is considered as very useful for heterogeneous land covers, common in very high-resolution satellite imagery because of their high spatial and low spectral resolution.

An object-based technique in eCognition® starts with a segmentation step: the image is subdivided into homogeneous regions based on their spectral characteristics, shape, scale (maximum allowed heterogeneity) and object hierarchy level (Giada et al., 2003). A high shape value corresponds with a low colour or spectral value due to the importance of shape compared to spectral characteristics and visa versa. With relation to shape, a weighting should be made between smoothness and compactness. The latter is high for objects different in shape, but with similar spectral characteristics. Discrete land cover types often show a difference in internal heterogeneity and, as a result, various segmentation levels with specific scale values should be used. Hence, a high internal heterogeneity corresponds to a high scale value. Segmentation starts at a pixel level where each pixel is considered as a separate object (Fig. 6). Subsequently, different pixels are grouped according to the parameters defined and a new level is generated based on the previous level (level 1 in Fig. 6). The segmented regions gradually become larger from one level to the next so that the internal heterogeneity of the objects increases (level 3 in Fig. 6). As a consequence, segmentation assumes that more heterogeneous surfaces are stretched out over larger areas.

In a second step (the classification step), training objects are selected to train the classification in analogy to the pixel-based classification, but instead of using pixels as training samples, objects (the result of the segmentation step) are used. Subsequently, classification parameters are defined. In comparison to a pixel-based classification, spectral, shape

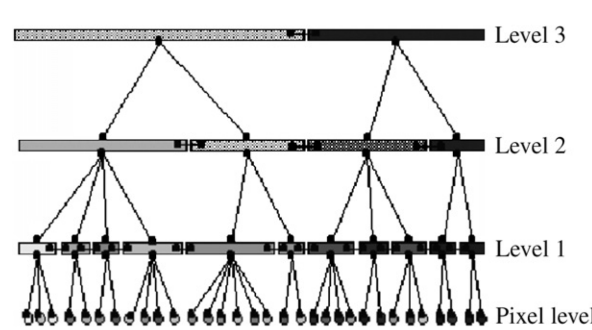

Fig. 6. Pixel aggregation within the segmentation procedure (Willhauck, 2000).

Table 3
Segmentation parameters (increasing pixel aggregation level from top to bottom)

Level	Scale factor	Homogeneity criteria		
		Shape factor	Compactness factor	Smoothness factor
1	5	0.023	0	1
2	10	0.07	0.85	0.15

and hierarchical parameters are taken into account (Table 3). Finally, a nearest neighbourhood classification is conducted (Baatz and Schäpe, 2000; Baatz et al., 2002).

4. Results

4.1. Visual interpretation

At Hisar, a distinction between archaeological structures and inferred archaeological structures based on the on the Ikonos-2 satellite image is made (Fig. 7). Only the main visual structures are indicated. The significance of the inferred structures is not yet clear. Also, colour and shape of these inferred archaeological structures are less characteristic. The identified objects are remnants of a Byzantine and Early Hellenistic defence wall and some pre-Roman house constructions (Waelkens et al., 2000). The perimeter of the inferred defence wall elements that are identified by visual interpretation amounts to 510 m. The remnants of ancient houses cover an area of 3800 m^2 and are subdivided into three zones.

The visual interpretation of the Ikonos-2 image is used to evaluate the information gathered by the different automatic extraction techniques (see Sections 4.2, 4.3, 4.4). The advantage of a visual interpretation derived from very high-resolution satellite imagery over a field survey is the ability to correlate archaeological structures and construct an initial city ground plan. The results of such interpretation are a useful document for guiding different types of archaeological field work.

4.2. Edge enhancement filtering technique

The initial result of the automatic extraction of archaeological features by edge enhancement is a greyscale image (Fig. 8a). This initial result is further reclassified according to values corresponding to archaeological features: 100–400 for non-shadow linear features and −70 to −400 for shadow linear features (Fig. 8b and c). The definition of these values is based on a visual interpretation of the Ikonos-2 image. The final result is an image with shadow and non-shadow lineaments in red and yellow (Fig. 8d). Unfortunately, these lineaments do not only show archaeological structures. Edge enhancement filtering clearly does not provide a unique class for archaeological features, which is at least partly due to the intermingling of archaeological remnants with other linear features such as rows of trees and shrubs. Trees and shrubs overgrowing archaeological remains represent a very normal situation for most Mediterranean sites where flocks of sheep and goats are forbidden. As a result one may suggest that filtering is not the best option for adequate archaeological feature extraction.

4.3. Pixel-based classification

After evaluation of several pixel-based techniques, we conclude that the maximum likelihood classification provides the best results. Fig. 9 shows the results of this maximum likelihood classification on which both the soft (Fig. 9a) and hard version (Fig. 9b) are shown. By using a soft (rule) classifier, we were able to set the minimum membership value for each class and steer the classification result in contrast with the procedure applied for the hard classifier.

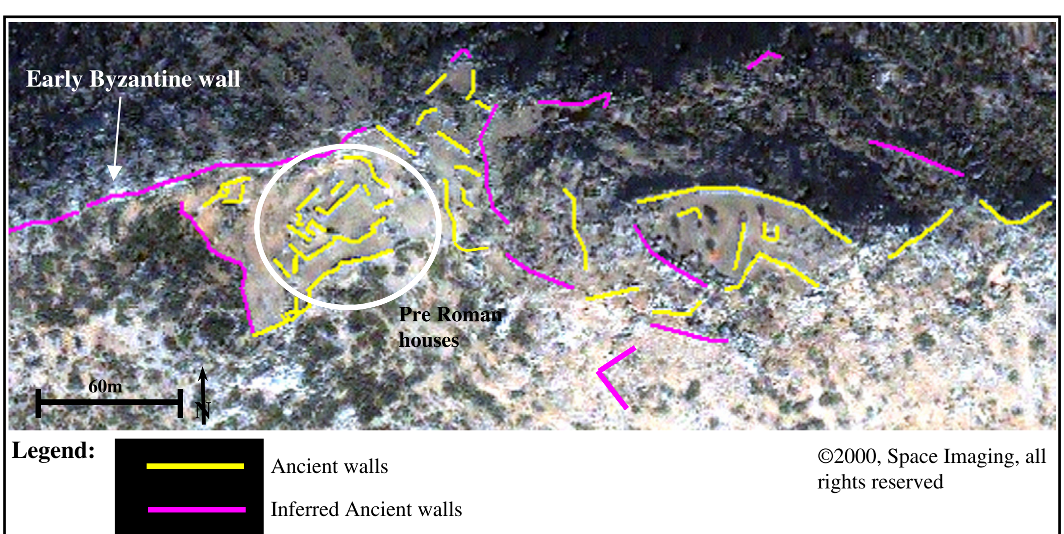

Fig. 7. Visual interpretation of main archaeological structures on Ikonos-2 imagery.

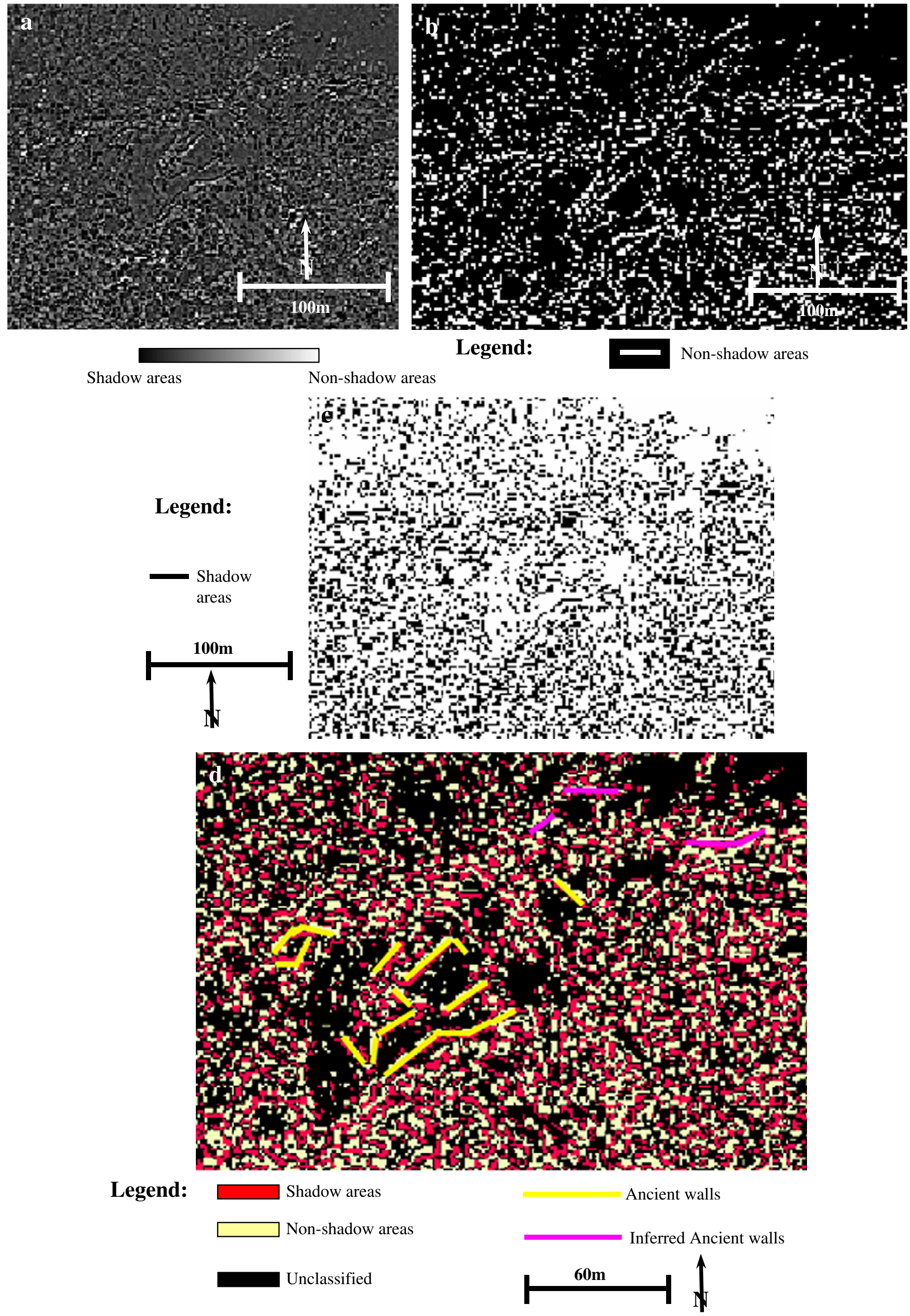

Fig. 8. Result edge enhancement filtering technique. (a) Initial result edge enhancement. (b) Non-shadow areas classification. (c) Shadow areas classification. (d) Final result edge enhancement filtering.

For classes with a high separability index, the application of a rule classifier generates good results. The results of shadow areas are acceptable; although a post classification threshold—e.g. on area—is necessary to extract areas under shadow directly connected to archaeological features.

Fig. 10 shows the membership value distribution of inferred limestone outcrops. The level of agreement between a pixel and the training sample of a category is expressed by a membership value, assigned to each pixel for each category. If the training sites are well chosen, many pixels will have the highest membership value. This is, however, not the case for limestone outcrops as the peak is shifted to the left and the signature mean is off-centre from the pixels it represents. There are two explanations for this kind of distributions: poor training samples or class heterogeneity. For limestone outcrops, the latter explanation is considered

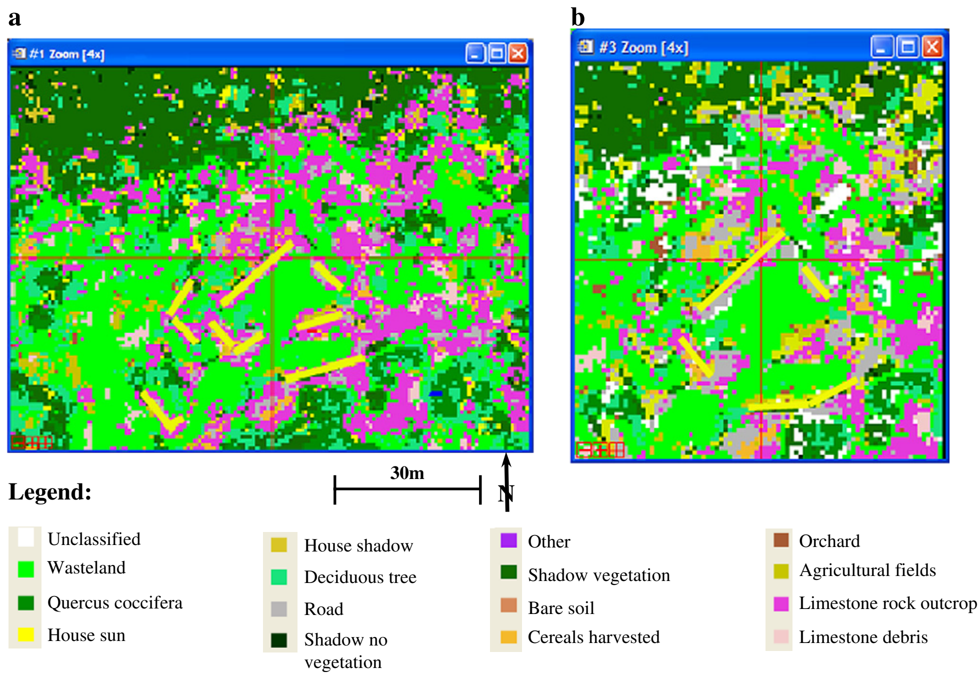

Fig. 9. Pixel-based maximum likelihood classification result. (a) Hard classifier version. (b) Soft classifier version.

most plausible. The spectral characteristics of limestone in the vicinity of Hisar are indeed very diverse due to surface weathering, mosses and lichens or internal chemical composition.

Due to separability index problems, the application of a rule (soft) classifier does not provide better results for classes that experience separability problems (e.g. many areas are mistakenly assigned to crops). Also, a mixture between evergreen and deciduous trees and shrubs occurs. Additionally, archaeological features are visible but they do not belong to a unique class as they should. The maximum likelihood classification accuracy without the application of a rule classifier amounts to 70%, whereas the accuracy of the application of a rule classifier drops to 40%.

4.4. Object-based classification

To cope with the imperfections of pixel-based methods, an object-based remote sensing technique, particularly developed for very high-resolution images, is applied (Blaschke and Strobl, 2001; Giada et al., 2003; Kiema, 2002).

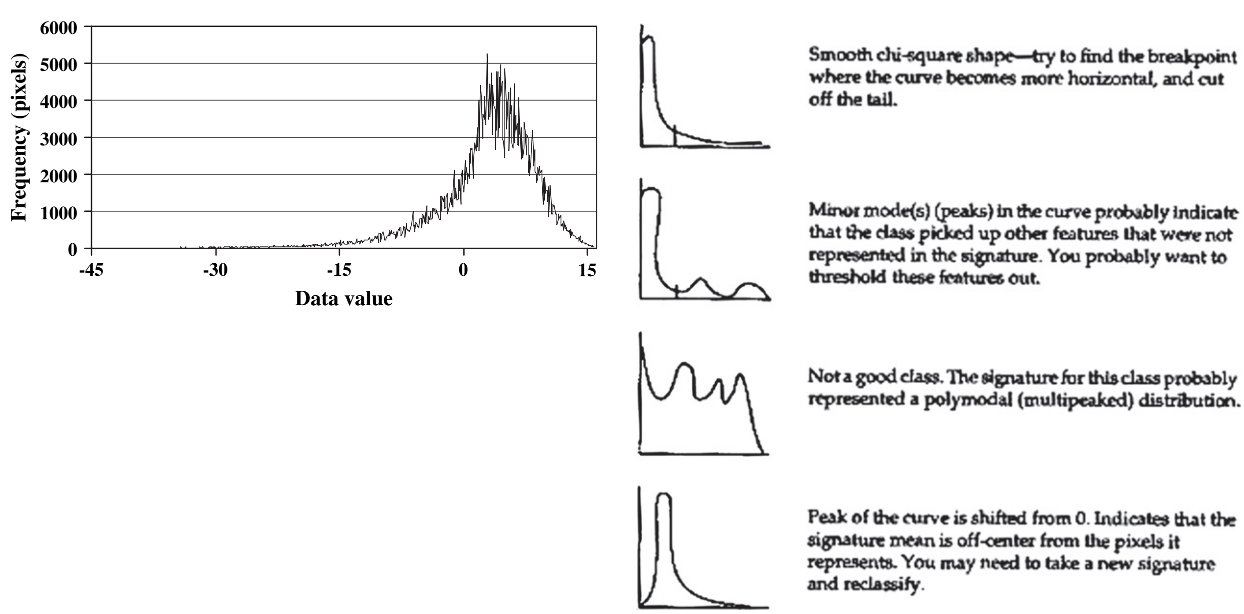

Fig. 10. Membership value distribution of limestone outcrops.

Similar to the pixel-based method, limestone outcrops and shadows of walls and other landscape features are selected to classify archaeological structures. For the segmentation of archaeological structures built with limestone blocks, a first segmentation level is used. For areas under a shadow, a second segmentation level is applied because they are more homogenous and less segment demanding. Segmentation parameters are presented in Table 3. Fig. 11 shows the results of the object-based classification of both limestone outcrops and areas under a shadow for the Hisar site. The results of the segmentation procedure of limestone outcrops (level 1 in Table 3) and areas under a shadow (level 2 in Table 3) are represented in Fig. 11a and b, respectively. The results of the classification procedure are depicted in Fig. 11c.

From Fig. 11 we conclude that many of the archaeological structures are well segmented and appear as separate objects. The classification results show that the differentiation of walls versus limestone and evergreen versus deciduous trees and shrubs works very well. For most landscape elements on very high-resolution images, object-based classification is very effective compared to other automatic extraction methods. By using an object-based classification technique, the accuracy increases to 80%. Unfortunately, the features within the classification category ‘‘shadows of walls and other landscape structures’’ (Fig. 11c) do not only belong to archaeological structures, but also to other objects, such as trees. By analogy, we observe that the category ‘‘limestone outcrops’’ (Fig. 11c) encompasses more than archaeological

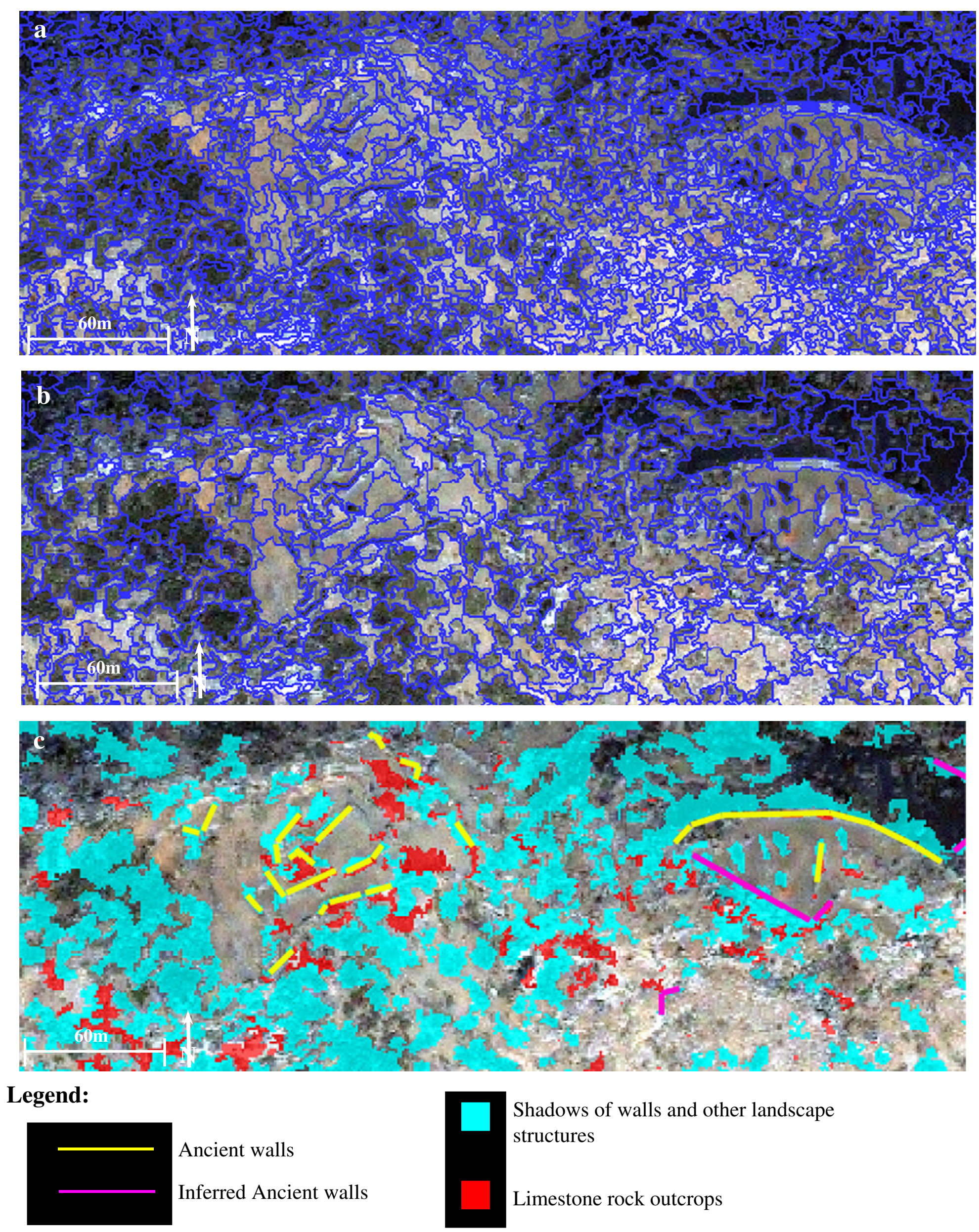

Fig. 11. Object-based segmentation and image classification results. (a) Segmentation level 1: limestone rock outcrops (i.e. archaeological features). (b) Segmentation level 2: shadows of walls and other landscape elements. (c) Classification result of both limestone rock outcrops and shadows of walls.

structures, as also fresh limestone outcrops are assigned to this category.

Because of the non-unique spectrum or shape characteristics of archaeological structures, object-based classification seems impossible. We are not able to achieve a unique class for archaeological features under a shadow and a class for archaeological features built in limestone.

The segmentation procedure within the object-based method is, however, a valuable means to limit the digitalisation of individual archaeological structures as performed in a visual interpretation.

5. Discussion and conclusion

The different automatic classification methods applied in this paper on very high-resolution images of the Hisar site recognise archaeological features with variable success. For most landscape elements, pixel-based techniques and especially object-based classification techniques provide reasonable results, but they do not result in a unique class for archaeological structures. For pixel-based techniques and to a lesser extend object-based techniques, this is primarily due to the spectral similarity between archaeological remains and the surrounding substrate, a coincidence that is seldom an issue for other landscape elements. Object-based classification methods are in addition hampered by the fact that most archaeological remains lack uniform shape characteristics relative to modern houses or trees. However, by taking into account shape characteristics, object-based techniques provide more satisfactory results relative to pixel-based techniques. Filtering does not provide a unique class for archaeological structures on the Hisar site and its contribution is not better than any other applied technique. This is due to the presence of many other types of linear features of various lengths and irregularity.

If the archaeological structures at Hisar should consist of materials different from those of the immediate surroundings, it is expected that the automatic extraction of archaeological features from very high-resolution remote sensing images would be more successful. Since the Hisar site is protected by the Turkish government, the lack of vegetation management and interdiction of herding flocks causes an expansion of shrubs and trees. With some on site vegetation maintenance, much of the areas under a shadow would disappear and the classification of archaeological features would be more straightforward. In an open field landscape, the automatic extraction would be far less complicated.

A visual interpretation of very high-resolution images presents satisfactory results. Such interpretation will provide information on site location, site extension or site planning and should precede archaeological field studies. We recommend conducting a visual interpretation before applying automatic extraction techniques. Although the existing automatic extraction techniques are not fully satisfactory, they should be further refined since they are less time consuming when applied on large areas and on sites with well visible structures. These methods are also less subjective than visual interpretation.

Possibilities for refining automatic extraction methods include improvements in the spectral and/or spatial resolution of the imagery. By increasing the spectral resolution without enhancing the spatial resolution of the imagery, classes will be better separated and few features will be assigned to an incorrect category. Improving the spatial resolution without increasing the spectral resolution will result in the visual identification of archaeological structures with more detail and assignment of a number of these detailed structures to the correct spectral class. It is not excluded, however, that the number of incorrectly assigned landscape features will increase, especially after the application of a pixel- or GIS-based classification method. As a result, the classification accuracy will therefore not necessarily increase. After enhancement of both the spatial and spectral resolution, an improvement in the classification accuracy is expected so that archaeological structures will be identified in more detail. Currently, the only possibility of improving both spatial and spectral resolution is the application of hyperspectral imagery with a very high spatial resolution (if possible <1 m), supplemented with LIDAR data (Challis, 2006; Devereux et al., 2005). A literature review (Buck et al., 2003) and spectroscopy measurements in the Hisar area show that hyperspectral imagery is able to identify locations with high ceramic densities so that relevant areas for field prospection can be delimited.

Acknowledgements

This research is supported by the Belgian Programme on Interuniversity Poles of Attraction initiated by the Belgian State, Prime Ministers Office, Science Policy Programming (IUAP P5/09). The authors would like to thank the entire archaeological team of the Sagalassos project for providing sufficient archaeological information in order to conduct this research.

References

Abrams, M., 2000. The Advanced Spaceborne Thermal Emission and Reflection Radiometer (ASTER): data products for the high spatial resolution imager on NASA's Terra Platform. International Journal of Remote Sensing 21 (5), 847–859.

Baatz, M., Schäpe, A., 2000. Multiresolution segmentation: an optimization Approach for high quality multi-scale image segmentation. In: Strobl, J., Blaschke, T. (Eds.), Angewandte Geographische Informations verarbeitung XII. Wichmann, Heidelberg, pp. 12–23.

Baatz, M., Heynen, M., Hofmann, P., Lingenfelder, I., Milmer, M., Schaepe, A., Weber, M., Willhauck, G., eCognition, 2002. Object Oriented Image Analysis, User guide (3.0). Definiens AG, Munich.

Blaschke, T., Strobl, J., 2001. What's wrong with pixels? Some recent developments interfacing remote sensing and GIS. GIS—Zeitschrift für Geoinformationssysteme 6, 12–17.

Bracke, H., 1993. Pisidia in Hellenistic Times (334-25B.C.). In: Waelkens, M. (Ed.), Sagalassos I. First general report on the survey (1986–1989) and excavations (1990–1991). Acta Archaeologica Lovaniensia Monographiae 5. Acta Archaeologica Lovaniensia Monographiae 5. Leuven University Press, Leuven, pp. 15–37.

Buck, P.E., Sabol, D.E., Gillespie, A.R., 2003. Sub-pixel artifact detection using remote sensing. Journal of Archaeological Science 30, 973–989.

Challis, K., 2006. Airborne Laser Altimetry in Alluviated Landscapes. Archaeological Prospection 13 (2), 103–127.

Changlin, W., Ning, Y., Yueping, N., Lin, Y., 2004. Environmental Study and Information Extraction of Archaeological Features with Remote Sensing Imagery in Arid Area of Western China, Proceedings of the International Conference on Remote Sensing Archaeology, Beijing.

Chavez, P.S., 1988. An improved dark-object subtraction technique for atmospheric scattering correction of multispectral data. Remote Sensing of Environment 24 (3), 459–479.

Clark, C.D., Garrod, S.M., Pearson, M.P., 1998. Landscape archaeology and remote sensing in southern Madagascar. International Journal of Remote Sensing 19 (8), 1461–1477.

Colby, J.D., 1991. Topographic normalization in rugged terrain. Photogrammetric Engineering and Remote Sensing 57 (5), 531–537.

Conese, C., Gilabert, M.A., Maselli, F., Bottai, L., 1993. Topographic normalization of tm scenes trough the use of an atmospheric correction method and digital terrain models. Photogrammetric Engineering and Remote Sensing 59 (12), 1745–1753.

Crippen, R., 1987. The regression intersection method of adjusted image data for band rationing. International Journal of Remote Sensing 8 (2), 137–155.

Dave, J.V., Bernstein, R., 1982. Effect of terrain orientation and solar position on satellite-level luminance observations. Remote Sensing of Environment 12 (1), 331–348.

Devereux, B.J., Amable, G.S., Crow, P., Cliff, A.D., 2005. The potential of airborne lidar for detection of archaeological features under woodland canopies. Antiquity 79, 648–660.

Emmolo, D., Franco, V., Lo Brutto, M., Orlando, P., Villa, B., 2004. Hyperspectral Techniques and GIS for Arechaeological Investigation, Proceedings of the XXth ISPRS congress on Geo-imagery Bridging Continents, Istanbul, Turkey.

Franklin, S.E., Giles, P.T., 1995. Radiometric processing of aerial satellite remote-sensing imagery. Computers and Geosciences 21 (3), 413–423.

Georgoula, O., Kaimaris, D., Tsakiri, M., Patias, P., 2004. From the aerial photo to high-resolution satellite image. Tools for the archaeological research, Proceedings of XXth ISPRS congress on Geo-imagery Bridging Continents, Istanbul, Turkey.

Giada, S., De Groeve, T., Ehrlich, D., 2003. Information extraction from very high-resolution satellite imagery over Lukole refugee camp, Tanzania. International Journal of Remote Sensing 24 (22), 4251–4266.

Hofmann, P., 2001. Detecting informal settlements from Ikonos image data using methods of object oriented image analysis—an example from Cape Town (South Africa). In: Jürgens, C. (Ed.), Remote Sensing of Urban Areas/Fernerkundung in urbanen Räumen. Regensburger Geographische Schriften, pp. 107–118.

Jensen, J.R., 1996. Introductory Digital Image Processing: A Remote Sensing Perspective. Prentice Hall, New Jersey.

Jensen, J.R., 2000. Remote Sensing of the Environment. An Earth Resource Perspective. Prentice Hall, New Jersey.

Jordan, G., Meijninger, B.M.L., Van Hinsbergen, D.J.J., Meulenkamp, J.E., Van Dijk, P.M., 2005. Extraction of morphotectonic features from DEMs: Development and applications for study areas in Hungary and NW Greece. International Journal of Applied Earth Observation and Geoinformation 7 (3), 163–182.

Kaufman, Y.J., 1989. The atmospheric effect on remote sensing and its correction. In: Asrar, G. (Ed.), Theory and Application of Optical Remote Sensing. John Wiley and Sons, pp. 336–429.

Kiema, J.B.K., 2002. Texture analysis and data fusion in the extraction of topographic objects from satellite imagery. International Journal of Remote Sensing 23 (4), 767–776.

Leica, 2002. Erdas Field Guide, sixth ed. Leica Geosystems, Atlanta.

Lillesand, T.M., Kiefer, R.W., Chipman, J.W., 2004. Remote Sensing and Image Interpretation. John Wiley and Sons, New York.

Massalabi, A., He, D.C., Bénié, G.B., Beaudry, E., 2004. Restitution of information under shadow in remote sensing high space resolution images: Application to Ikonos data of Sherbrooke City, XXth ISPRS congress on Geo-Imagery Bridging Continents, Istanbul, Turkey.

Masuoka, P.M., Claborn, D.M., Andre, R.G., Nigro, J., Gordon, S.W., Klein, T.A., Kim, H., 2003. Use of Ikonos and Landsat for malaria control in the Republic of Korea. Remote Sensing of Environment 88, 187–194.

Mather, P.M., 2004. Computer Processing of Remotely-Sensed Images: An Introduction. John Wiley and Sons, Chichester.

Moore, G.K., Waltz, F.A., 1983. Objective procedures for lineament enhancement and extraction. Photogrammetric Engineering and Remote Sensing 49, 641–647.

Neawsuparp, K., Charusiri, P., 2004. Lineaments Analysis Determined from Landsat Data Implications for Tectonic Features and Mineral Occurrence in Northern Loei Area, NE Thailand. Science Asia 30, 269–278.

Pavlidis, L., 2005. High resolution satellite imagery for archaeological application www.fungis.org/files/news_mar05_archaeology.pdf.

PCI Geomatics, 1998. OrthoEngine reference manual. PCI Geomatics, Ontario.

Qi, J., Huete, A.R., Moran, M.S., Chehbouni, A., Jackson, R.D., 1993. Interpretation of vegetation indices derived from multi-temporal SPOT images. Remote Sensing of Environment 44 (1), 80–101.

Richards, J.A., Xiuping, J., 1999. Remote Sensing Digital Image Analysis An Introduction. Springer, New York.

Şenel, M., 1997. 1:100 000 scale geological maps of Isparta—J11 Quadrangle. General Directorate of Mineral Research and Exploitation, Ankara.

Sever, T.L., 1995. Remote Sensing. In: McGovern, P.E., Sever, T.L., Myers, J.W., Myers, E.E., Bevan, B., Miller, N.F., Bottema, S., Hongo, H., Meadow, R.H., Kuniholm, P.I., Bowman, S.G.E, Leese, M.N., Hedges, R.E.M., Matson, F.R., Freestone, I.C., Vaughan, S.J., Henderson, J., Vandiver, P.B., Tumosa, C.S., Beck, C.W., Smith, P., Child, A.M., Pollard, A.M., Thuesen, I., Sease, C. (Eds.), Science in Archaeology. American Journal of Archaeology 99 (1), 83–84.

Smith, J.A., Lin, T.L., Ranson, K.J., 1980. The Lambertian Assumption and Landsat Data. Photogrammetric Engineering and Remote Sensing 46 (9), 1183–1189.

Swain, P.H., Davis, S.M., 1978. Remote Sensing: The Quantitative Approach. McGraw Hill, New York.

Van Der Meer, F.D., De Jong, S., 2003. Imaging Spectrometry. Basic Principles and Prospective Applications. Kluwer Academic Publishers, Dordrecht.

Vanhaverbeke, H., Waelkens, M., 2003. The Chora of Sagalassos (Pisiadia, southwest Turkey). The Evolution of the Settlement Pattern from Prehistory until Recent Times. Brepols Publishers, Turnhout.

Vermeulen, F., Verhoeven, G., 2004. The contribution of aerial photography and field survey to the study of urbanization in the Potenza valley (Picenum). Journal of Roman Archaeology 17, 57–82.

Waelkens, M., Paulissen, E., Van Haverbeke, H., Öztürk, I., De Cupere, B., Ekinci, H.A., Vermeersch, P., Poblome, J., Degeest, R., 1997. The 1994 and 1995 Surveys on the territory of Sagalassos. In: Waelkens, M., Poblome, J. (Eds.), Sagalassos IV, Report on the Survey and Excavation Campaigns of 1994 and 1995. Acta Archaeologica Lovaniensia Monographiae 9. Leuven University Press, Leuven, pp. 11–103.

Waelkens, M., Vanhaverbeke, H., Paulissen, E., Poblome, J., Reyniers, J., Viane, W., Deckers, J., Decupere, B., Van Neer, W., Ekinci, H.A., Erbay, M.O., 2000. The 1996 and 1997 survey season at Sagalassos. In: Waelkens, M., Loots, L. (Eds.), Sagalassos V, Report on the Survey and Excavation Campaigns of 1996 and 1997. Acta Archaeologica Lovaniensia Monographiae 11A. Leuven University Press, Leuven, pp. 17–216.

Willhauck, G., 2000. Comparison of object oriented classification techniques and standard image analysis for the use of change detection between SPOT multispectral satellite images and aerial photos, Proceedings of the XIXth ISPRS congress, Amsterdam.